

Supporting Information for

Synthesis of core/shell Co-doped Rutile TiO₂ nanorods for MB degradation under visible light

Lang Yang,^a Jialei Ying,^a Zhenzhong Liu,*^a Guangyu He,^b Linli Xu,^c Mingyue Liu,^c Xinlei Xu,^a Guihua Chen,^c Meili Guan*^d

^aTaizhou Key Laboratory of Medical Devices and Advanced Materials, Taizhou Institute of Zhejiang University, Taizhou 318000, China

^bDepartment of Chemistry, School of Science and Research Center for Industries of the Future, Westlake University, Hangzhou 310030, China

^cSchool of Pharmaceutical and Chemical Engineering, Taizhou University, Taizhou 318000, China

^dCollege of Chemical and Biological Engineering, Shandong University of Science and Technology, Qingdao 266590, China

* Corresponding authors

E-mail addresses: zzliu@zju.edu.cn (Z.Z. Liu), mlguan@sdu.edu.cn (M.L. Guan).

Experimental Section:

The standard working curve of MB solution

A serials of MB solutions (5.0 mg L^{-1} , 10.0 mg L^{-1} , 15.0 mg L^{-1} , 20.0 mg L^{-1}) were prepared, and the absorbance was measured on UV-Vis spectrophotometer. The deionized water was used as the reference, and the absorbance at 662 nm was taken to draw the standard working curve.

Zeta potential measurements of Co-doped TiO₂ nanorods

The zeta potential were performed using a Zetasizer nano. The measurement is based on recording the electrophoretic mobilities of Co-doped TiO₂ nanorods in distilled water. Zeta potential was measured for pH=7 at $20 \text{ }^{\circ}\text{C}$ for several times.¹⁻²

Theoretical calculations by density functional theory (DFT)

To further explore the mechanism of adsorption, we carried out quantum chemical calculations using density functional theory (DFT). The structures of dyes were optimized using Gaussian 16 program package1 at B3LYP-D3(BJ)/6-31G* level,³⁻¹¹ and the wave functions were obtained at B3LYP-D3(BJ)/6-311G** level (B3LYP-D3(BJ)/6-311++G** level for anion)¹²⁻¹⁶ in solution, respectively. No imaginary frequency was found through frequency analysis for the optimized structures. The electrostatic potential and size are obtained with Multiwfn.

Data analysis:

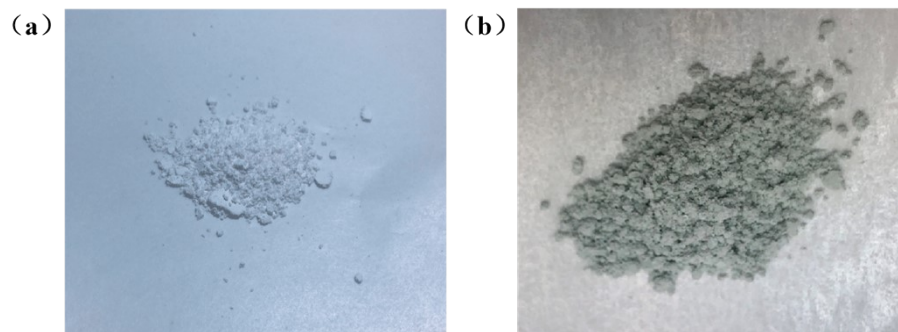


Fig. S1 The photographs of (a) pure rutile TiO_2 nanorods and (b) Co-doped rutile TiO_2 nanorods.

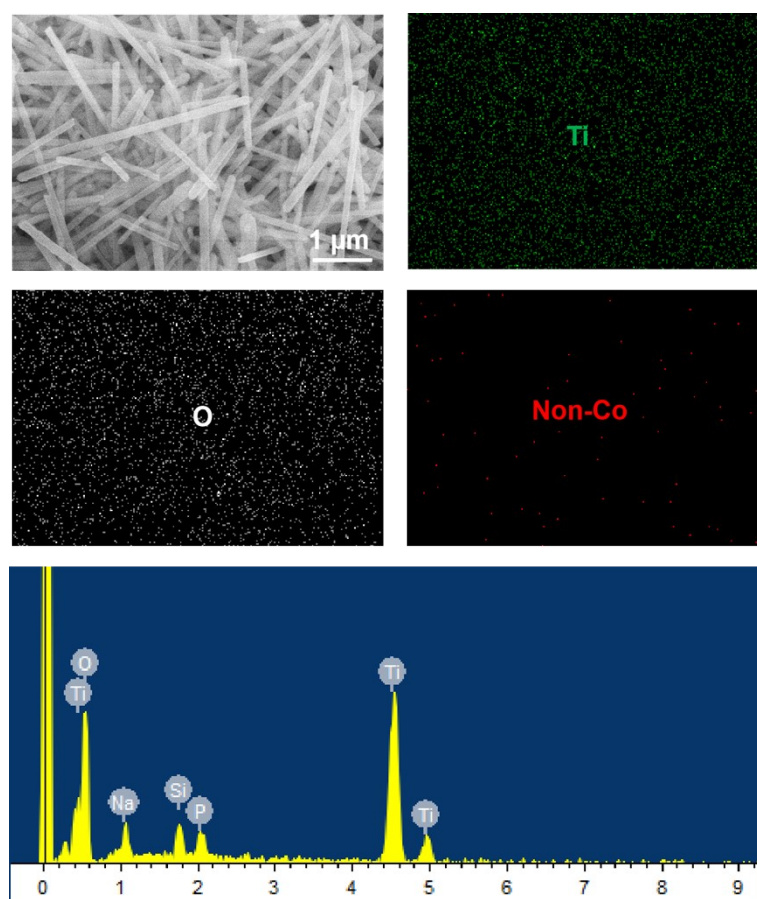


Fig. S2 The SEM image, EDS mapping and energy spectra of pure rutile TiO_2 nanorods with Ti, O elements.

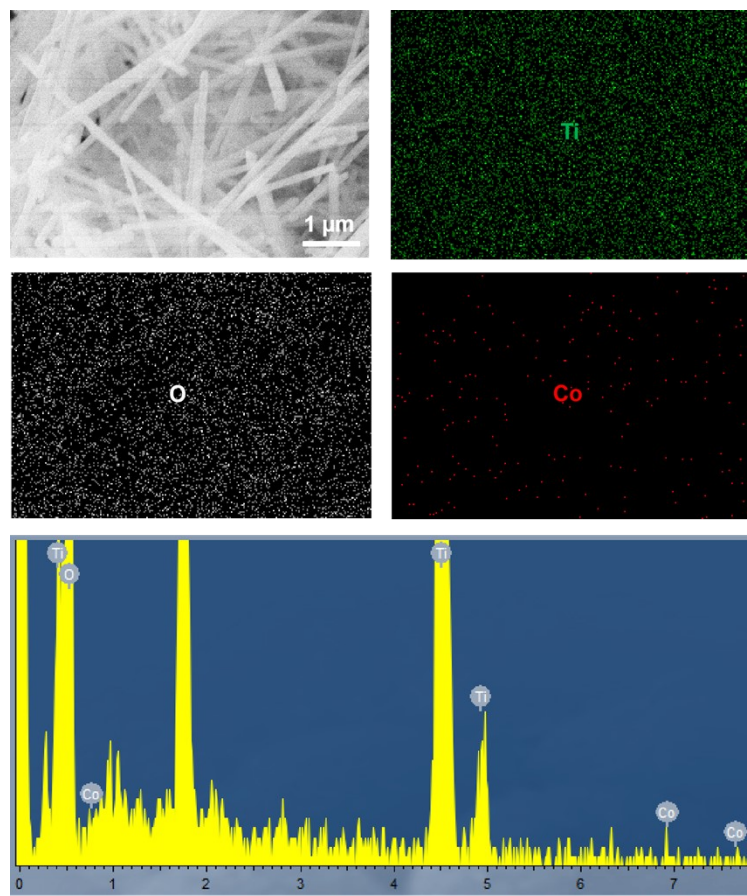


Fig. S3 The SEM image, EDS mapping and energy spectra of Co-doped rutile TiO_2 nanorods with Ti, O, Co elements.

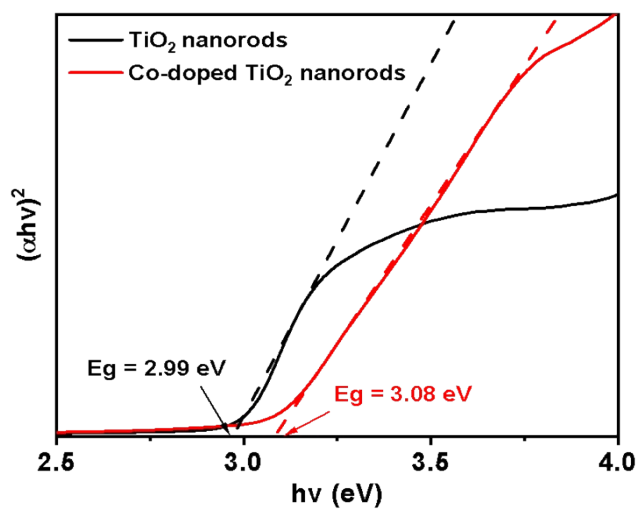


Fig. S4 The bandgap value estimated by a related curve of $(\alpha h\nu)^2$ versus photon energy plotted.

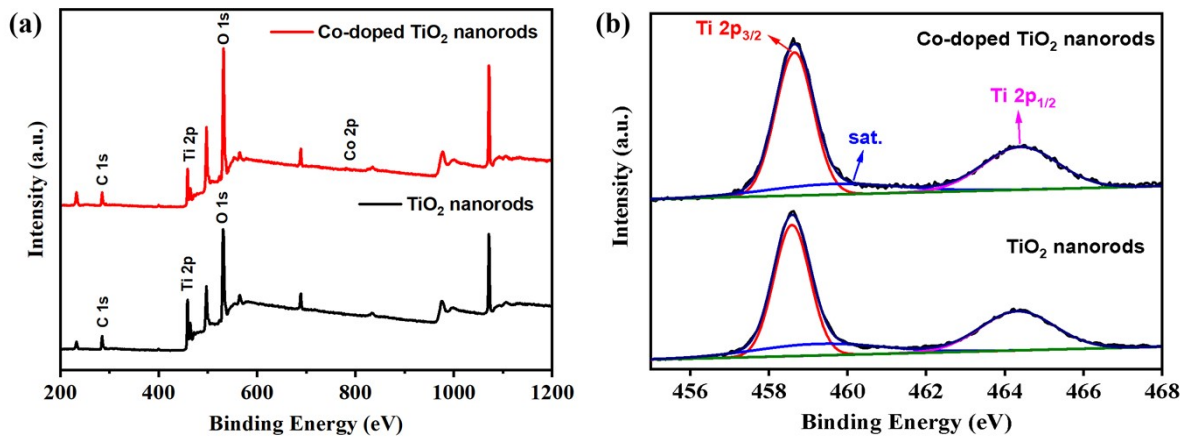


Fig. S5 (a) XPS wide spectra, (f) Ti 2p XPS spectra of TiO₂ nanorods and Co-doped TiO₂ nanorods.

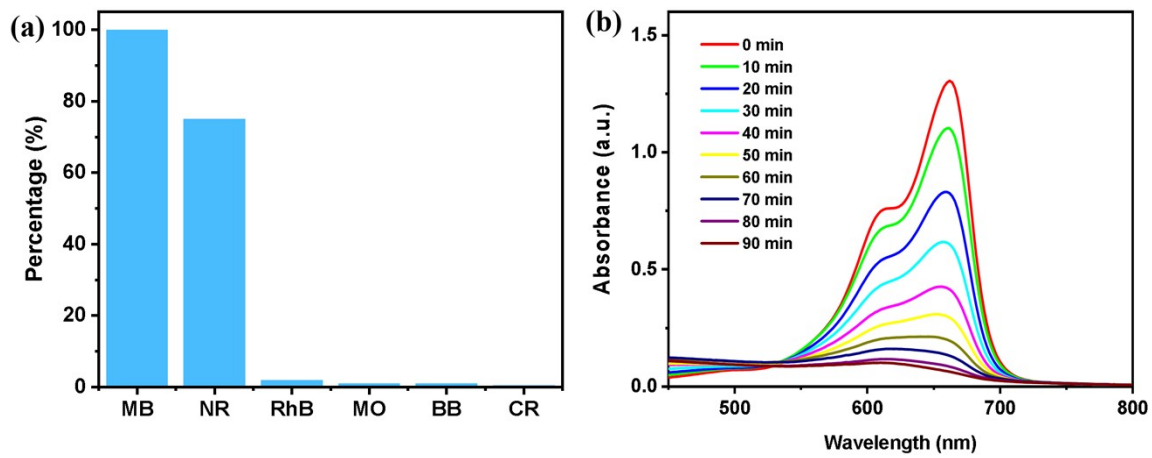


Fig. S6 Adsorption characteristics of Co-doped TiO₂ nanorods: (a) histogram of the selective adsorption capacities of different organic dyes, (b) UV-Vis absorption spectra of MB solution over 90 min.

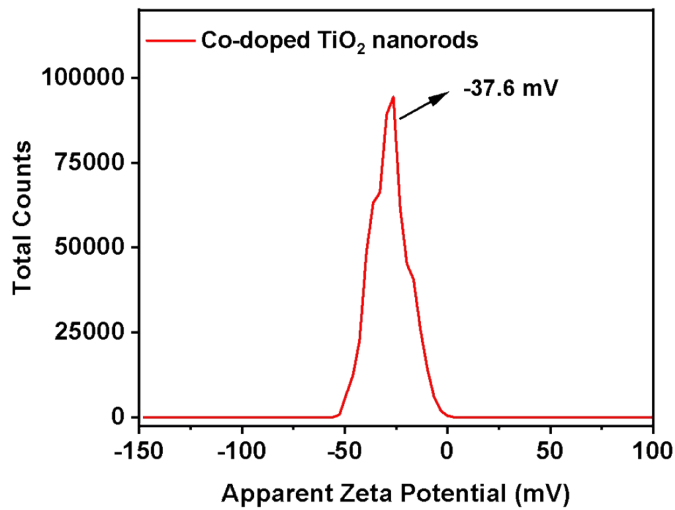


Fig. S7 The zeta potential distribution of Co-doped TiO₂ nanorods in water.

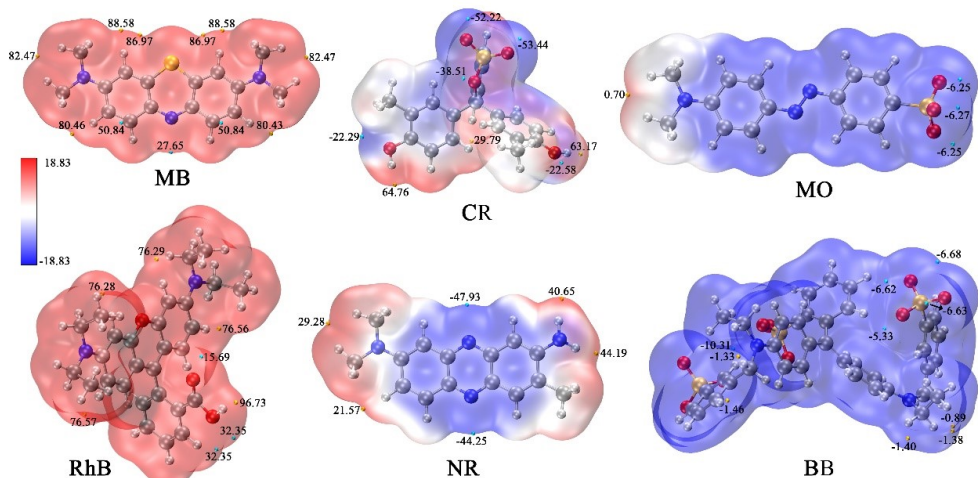


Fig. S8 Electrostatic potential distributions on the van der Waals surfaces (isodensity = 0.001 a.u.) of six dyes are illustrated. A subset of extremal points of the electrostatic potential is highlighted with yellow and cyan markers, where yellow indicates local maxima and cyan indicates local minima (The values are expressed in units of kcal/mol).

Table 1 The size features of six dyes.

Dyes \ Size	MB	CR	MO	RhB	NR	BB
Å	16.6*7.9*4.2	13.7*11.4*9.1	17.4*7.2*5.3	17.3*13.8*9.2	15.0*8.1*4.2	19.3*13.2*10.4

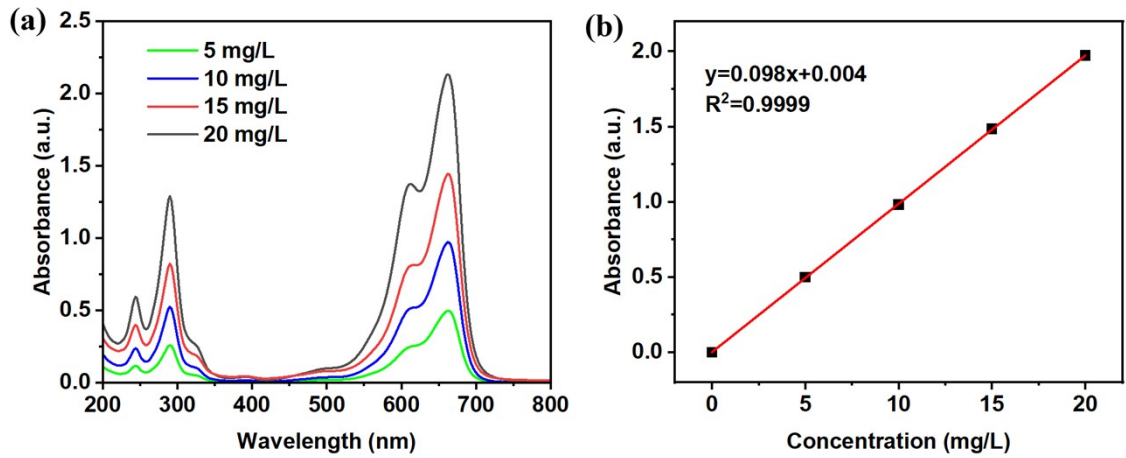


Fig. S9 (a) UV-Vis absorption spectra of MB solution with different concentrations and (b) the curvilinear regression curve of absorbance as a function of MB concentration.

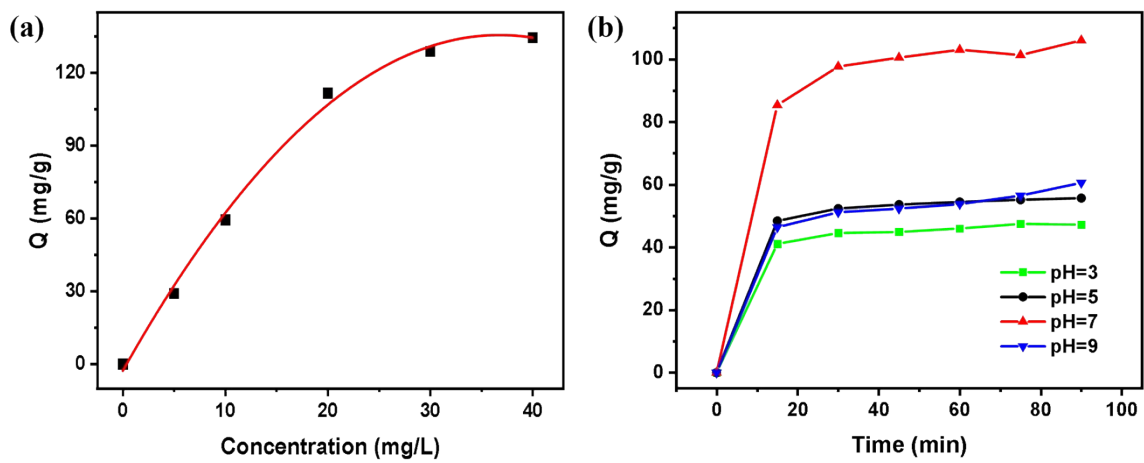


Fig. S10 Adsorption characteristics of Co-doped TiO₂ nanorods: (a) adsorption isotherms of MB at various initial concentrations, (b) adsorption performance of MB at different pH levels.

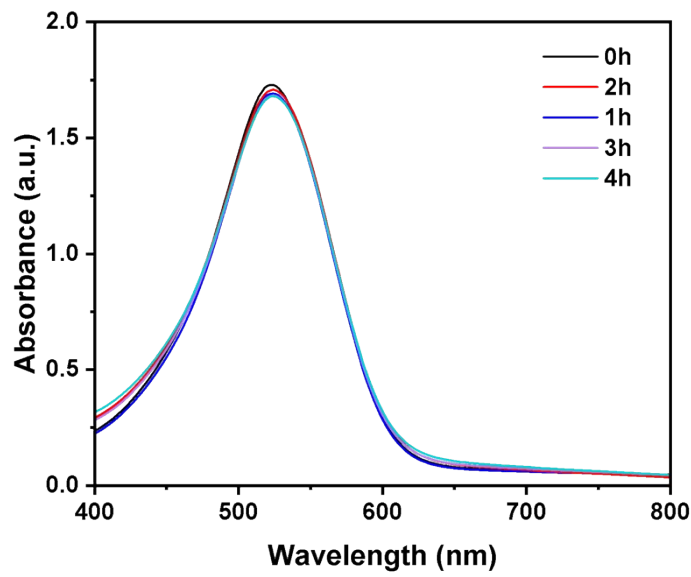


Fig. S11 The UV-Vis spectra of neutral red (NR) solution using Co-doped TiO₂ nanorods under visible light at different times.

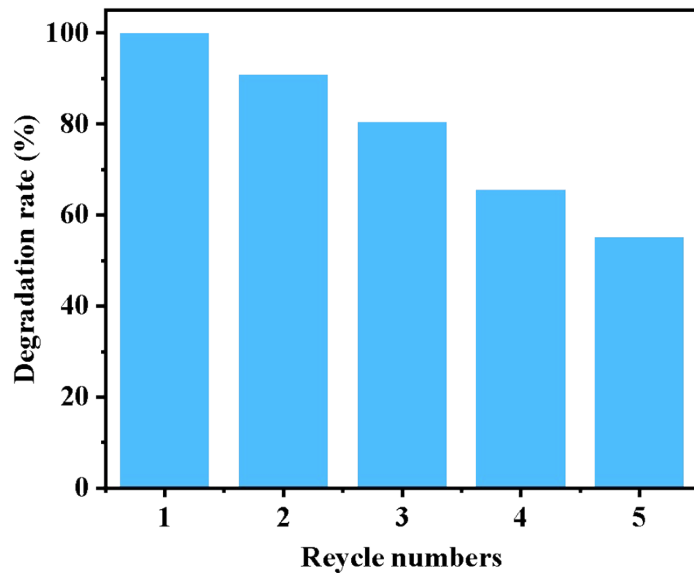


Fig. S12 The Repeated photocatalytic degradation of MB solution under visible light for 5 times.

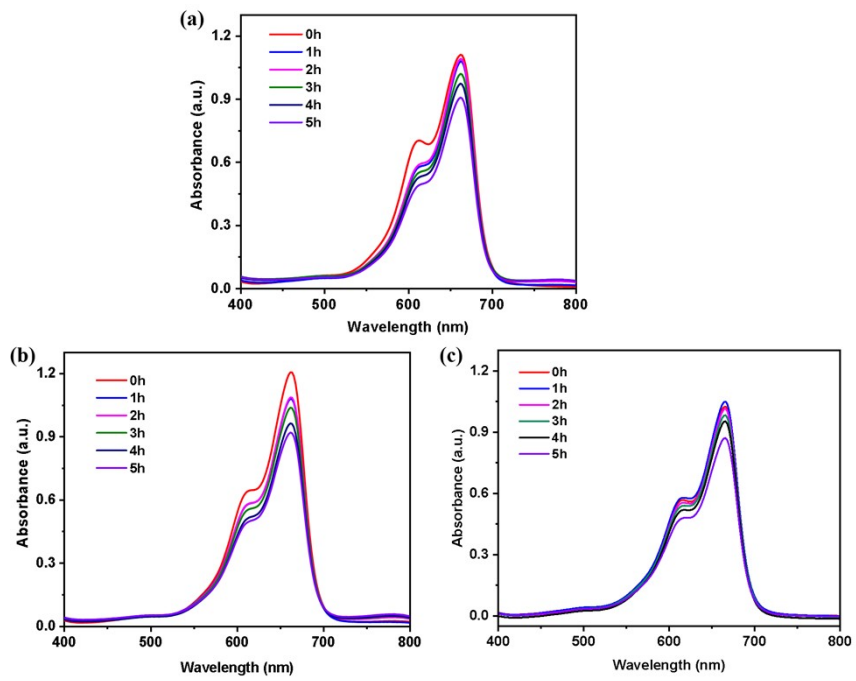


Fig. S13 The UV-Vis spectra of degradation of MB at different (a) pH=3, (b) pH=5 and (c) pH= 9 by Co-doped TiO₂ nanorods under visible light.

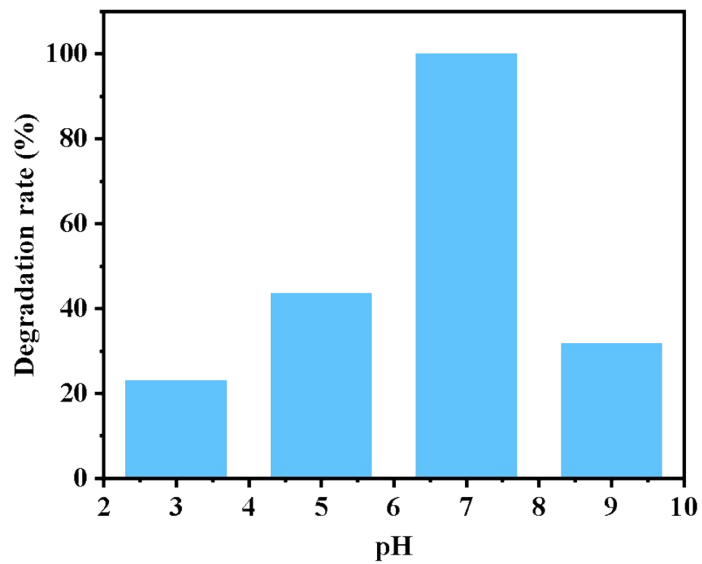


Fig. S14 The degradation rate of MB solution at different pH values: pH=3, pH=5, pH=7, and pH=9 by Co-doped TiO₂ nanorods under visible light.

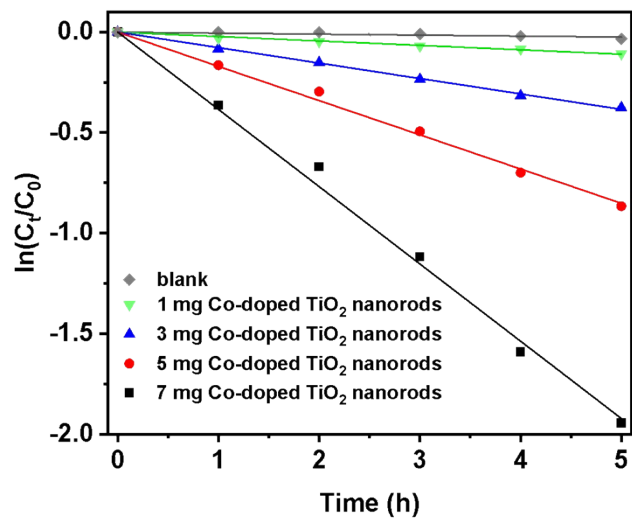


Fig. S15 The degradation of MB solution with different contents of Co-doped TiO_2 nanorods under visible light.

References:

1. Bukackova M.; Rusnok P.; Marsalek R. Mathematical Methods in the Calculation of the Zeta Potential of BSA. *J. Solution Chem.*, 2018, 47: 1942–1952.
2. Laia Ginés, Soumen Mandal, Ashek-I-Ahmed, Chia-Liang Cheng, Maabur Sowc, Oliver A. Williams, Positive zeta potential of nanodiamonds. *Nanoscale*, 2017, 9:12549-12555.
3. Gaussian 16, Revision C.01, M. J. Frisch, G. W. Trucks, H. B. Schlegel, G. E. Scuseria, M. A. Robb, J. R. Cheeseman, G. Scalmani, V. Barone, G. A. Petersson, H. Nakatsuji, X. Li, M. Caricato, A. V. Marenich, J. Bloino, B. G. Janesko, R. Gomperts, B. Mennucci, H. P. Hratchian, J. V. Ortiz, A. F. Izmaylov, J. L. Sonnenberg, D. Williams-Young, F. Ding, F. Lipparini, F. Egidi, J. Goings, B. Peng, A. Petrone, T. Henderson, D. Ranasinghe, V. G. Zakrzewski, J. Gao, N. Rega, G. Zheng, W. Liang, M. Hada, M. Ehara, K. Toyota, R. Fukuda, J. Hasegawa, M. Ishida, T. Nakajima, Y. Honda, O. Kitao, H. Nakai, T. Vreven, K. Throssell, J. A. Montgomery, Jr., J. E. Peralta, F. Ogliaro, M. J. Bearpark, J. J. Heyd, E. N. Brothers, K. N. Kudin, V. N. Staroverov, T. A. Keith, R. Kobayashi, J. Normand, K. Raghavachari, A. P. Rendell, J. C. Burant, S. S. Iyengar, J. Tomasi, M. Cossi, J. M. Millam, M. Klene, C. Adamo, R. Cammi, J. W. Ochterski, R. L. Martin, K. Morokuma, O. Farkas, J. B. Foresman, and D. J. Fox, Gaussian, Inc., Wallingford CT, 2019.
4. Stephens P. J.; Devlin F. J.; Chabalowski C. F.; Frisch M. J., Ab Initio Calculation of Vibrational Absorption and Circular Dichroism Spectra Using Density Functional Force Fields. *The Journal of Physical Chemistry* 1994, 98 (45): 11623-11627.
5. Grimme S.; Antony J.; Ehrlich S.; Krieg H. A Consistent and Accurate Ab Initio Parametrization of Density Functional Dispersion Correction (DFT-D) for the 94 Elements H-Pu. *J. Chem. Phys.*, 2010, 132 (15), 154104.
6. Grimme S.; Ehrlich S.; Goerigk L. Effect of the Damping Function in Dispersion Corrected Density Functional Theory. *J. Comput. Chem.*, 2011, 32 (7): 1456–1465.
7. Ditchfield R., Hehre W. J., Pople J. A. Self-Consistent Molecular-Orbital Methods. IX. An Extended Gaussian-Type Basis for Molecular-Orbital Studies of Organic Molecules. *J. Chem. Phys.*, 1971, 54: 724-728.
8. Franc Michèle M., Pietro William J., Hehre Warren J., Binkley J. Stephen, Gordon Mark S., DeFrees Douglas J., Pople John A. Self-consistent molecular orbital methods. XXIII. A polarization-type basis set for second-row elements. *J. Chem. Phys.*, 1982, 77: 3654-3665.
9. Gordon Mark S., Binkley J. Stephen, Pople John A., Pietro William J., Hehre Warren J. Self-consistent molecular-orbital methods. 22. Small split-valence basis sets for second-row elements. *J. Am. Chem. Soc.*, 1982, 104: 2797-2803.
10. Hariharan P. C., Pople J. A. The influence of polarization functions on molecular orbital hydrogenation energies. *Theor. Chim. Acta*, 1973, 28: 213-222.
11. Hehre W. J., Ditchfield R., Pople J. A. Self-Consistent Molecular Orbital Methods. XII. Further Extensions of Gaussian-Type Basis Sets for Use in Molecular Orbital Studies of Organic Molecules. *J. Chem. Phys.* 1972, 56: 2257-2261.
12. Clark Timothy, Chandrasekhar Jayaraman, Spitznagel Günther W., Schleyer Paul Von Ragué. Efficient diffuse function-augmented basis sets for anion calculations. III. The 3-21+G basis set for first-row elements, Li-F. *J. Comput. Chem.*, 1983, 4: 294-301.
13. Franc Michèle M., Pietro William J., Hehre Warren J., Binkley J. Stephen, Gordon Mark S., DeFrees

- Douglas J., Pople John A. Self-consistent molecular orbital methods. XXIII. A polarization-type basis set for second-row elements. *J. Chem. Phys.*, 1982, 77: 3654-3665.
- 14. Krishnan R., Binkley J. S., Seeger R., Pople J. A. Self-consistent molecular orbital methods. XX. A basis set for correlated wave functions. *J. Chem. Phys.*, 1980, 72: 650-654.
 - 15. McLean A. D., Chandler G. S. Contracted Gaussian basis sets for molecular calculations. I. Second row atoms, Z=11-18. *J. Chem. Phys.* 1980, 72: 5639-5648.
 - 16. Spitznagel Günther W., Clark Timothy, Schleyer Paul von Ragué, Hehre Warren J. An evaluation of the performance of diffuse function-augmented basis sets for second row elements, Na-Cl. *J. Comput. Chem.*, 1987, 8: 1109-1116.